NOTICE

CERTAIN DATA CONTAINED IN THIS DOCUMENT MAY BE DIFFICULT TO READ IN MICROFICHE PRODUCTS.

ATOMIC-SCALE SIMULATION OF ADHESION BETWEEN METALLIC SURFACES

PAUL A. TAYLOR
Sandia National Laboratories, P.O. Box 5800, Albuquerque, NM 87185

SAND--90-3057C

DE91 004722

ABSTRACT

We have performed MD simulations of adhesive phenomena, on an atomic scale, between metals possessing both smooth and stepped-surfaces. Studies of adhesion between identical metals, consisting of either Au, Cu, or Ni, with (001) or (111) orientations, reveal the existence of adhesive avalanches as the bodies are brought to within a critical separation (~2 Å). That is, as the surfaces approach one another, one or both surface layers becomes unstable, and abruptly moves towards the other. This signals a transition from an initial system with two distinct surfaces to one possessing no identifiable surfaces. The presence of adhesive avalanches will pose difficulties in determining adhesive forces and energies by means of atomic force microscopy at sub-nanometer separations of probe tip and sample surface.

INTRODUCTION

The study of adhesion between metals, semiconductors, glasses, etc., is becoming increasingly more urgent as technological advances rely upon the ability to fabricate devices on smaller length scales (e.g., nanostructures). Phenomena such as friction and wear involve the formation and destruction of adhesive interfaces. Unfortunately, since adhesion involves the formation of a buried interface, it is difficult to study experimentally. Current state-of-the-art experimental techniques to study adhesion have relied primarily on atomic force microscopy (AFM) [1]. Basically, AFM involves the movement of an atomic-size probe tip over a sample surface to determine a constant force contour, reflecting, in some sense, on the topology of the sample surface. The advantage of AFM over related techniques, such as scanning tunneling microscopy, is that the tip and sample need not be conductors, and thus, a wider range of applications is possible. AFM has more recently been applied to the study of adhesive forces between various materials from metals to insulators [2-5]. These works have employed AFM to basically measure the interfacial force between an AFM probe tip and sample surface as a function of interfacial separation. Integration of the experimentally measured force data from infinite separation could, in principle, allow the adhesive energy to be determined as a function of the separation. Thus, this technique would appear to be a useful quantitative tool for study and analysis of surface and interfacial energetics.

To date, we have performed atomistic simulations of adhesive phenomena between smooth and stepped-surfaces of identical metals of either Au, Cu, or Ni with (001) or (111) orientations. In all cases, the presence of adhesive avalanches were predicted. First coined by Smith et al [6], an "adhesive avalanche" is predicted whenever strongly interacting surfaces approach one another, where one or both of the surface layers becomes unstable, signaling an abrupt transition from an initial system consisting of two distinct structures with interacting surfaces to a single, strained structure possessing no identifiable surfaces. The presence of adhesive avalanches should cause difficulties in the measurement of adhesive forces by means of AFM techniques and the interpretation of those results to yield adhesion energies. That is, as the AFM probe tip is vertically manipulated in an attempt to yield a force vs. separation curve, the onset of an avalanche, at a critical value of separation, will cause the probe tip to abruptly approach the sample surface, effectively creating a range of forbidden separation values in which adhesive force determination would be impossible. In addition, our results show that

an avalanche event results in the generation of an adhesive force spike only picoseconds in duration, and therefore not detectable using current experimental techniques. Consequently, any attempt to interpret experimental AFM data to determine adhesive energies will, by oversight of the energy associated with an avalanche event, arrive at misleading results. These difficulties are outlined in greater detail later in the paper.

METHODOLOGY

The objective of the present study is to examine the adhesive phenomena between metals by means of atomic-scale simulation for a number of different metals, crystallographic orientations, and surface geometries. In particular, gold, copper, and nickel were chosen since their structural energetics are represented reasonably well by the embedded-atom method (EAM) [7]. The EAM model of atomic interactions retains enough of the bonding physics to be accurate over a wide range of problems, including surfaces, interfaces, and defects.

The geometry for the smooth-surface simuations is schematically represented in Fig. 1a, whereas that for the stepped-surface geometry is shown in Fig. 1b. In both cases, the sample and tip are composed of the same material with their interacting surfaces being either the (111) or (001) crystallographic planes, and initially in structural registry. In the smooth-surface geometry, the tip and sample structures each possess three nondeformable (fixed) atomic planes which act as rigid mounts for manipulation and provide extended bulk-like environment for the moving planes. The deformable portions are each represented by four moving (deformable) planes of atoms. Both tip and sample structures possess a cross-section of 4 by 5 atoms (12.8 Å x 13.3 Å) in atomic planes parallel to the surface planes. Periodic boundary conditions are imposed on the lateral boundaries so that the model simulates a pair of infinite, parallel, smooth-surfaces in close proximity.

The stepped-surface simulations require a system possessing a greater number of atoms in order to approximate two bulk-like structures with one displaying a surface possessing an island structure consisting of a finite-size atomic monolayer (i.e., partial plane). Here, the tip is composed of seven full atomic planes of 12 by 14 atoms (30.7 Å x 31.0 Å) in cross-section, the uppermost one of which is rigid for manipulation purposes, and a 15 Å diameter partial plane consisting of 30 atoms centered on the lowermost full atomic plane (see Fig. 1b). The sample structure is comprised of seven atomic planes of 12 by 14 atoms in cross-section, with the bottom plane fixed. Periodic boundary conditions are enforced on the lateral boundaries for all but the partial atomic plane.

In both simulations, the tip and sample structures are initially placed within a proximal distance of one another such that structural relaxation (via molecular dynamics) of the respective surfaces proceeds without interference from the adjacent structure. This is accomplished by setting the inital rigid mount separation D such that the corresponding interfacial spacing d was at least 2.5 Å prior to relaxation. Interfacial separation d is defined as the distance separating the nearest adjacent atomic planes of the tip and surface structures beyond bulk separation. The rigid mount separation D is the distance separating the respective groups of rigid atomic planes in the tip and surface. After the initial relaxation procedure is completed, the tip and sample rigid mounts are set to approach one another at a constant rate of 0.1 Å/ps, eliminating the initial interfacial separation, and continuing until a minimum in the structural energy is encountered. In order to identify hysteretic effects, the rigid mounts are then set to move apart (at 0.1 Å/ps) until crystallographic failure is detected. The simulations employ molecular dynamics techniques and the EAM to determine the structural response of the system. A viscous term is included to dampen

transient oscillations. The simulations tracked the evolution of the structural state, along with the associated energetics, as the adhesive interactions changed in response to changes in the rigid mount separation D.

SIMULATION RESULTS

Simulation results were predicted for the adhesive responses of Au, Cu, and Ni, and found to be qualitatively similar. That is, except for displaying different critical separation values and corresponding energy changes at the onset of avalanche, the behavior of the three metals is identical. Therefore, due to paper length restrictions, we focus on the simulation results of a single, representative system: Cu(111).

Figs. 2a, 2b, and 2c display the interfacial separation d, structural energy E, and adhesive force F as functions of rigid mount separation D for the smooth-surface case. Here, the absissa values in the figures reflect the rigid mount separation minus the initial lengths of the tip and sample structures. On the approach leg, starting at D=2.5 Å and proceeding towards smaller D values, d~D, with E and F fairly constant until the onset of avalanche, occurring at D~1.8 Å. At this point, the interfacial separation abruptly decreases to a few tenths of angstroms, the energy falls precipitously to a lower value, and the force displays a spike profile, increasing 40-fold and decaying to a nominal value within a few picoseconds. The avalanche places d, E, and F on tracks that are distinct from their pre-avalanche profiles in an manner somewhat analogous to that of a 1st-order structural phase transition. In fact, these indicators signal the transition of two separate bodies into a single, strained structure. The oscillations in d, E, and F are a result of avalanche-induced wave motion that propagates back and forth in the newly-formed structure between the rigid mounts. Decreasing D further relieves the post-avalanche strain until the zero strain state is reached at D=0.

In the post-avalanche regime, at $D < 1.7$ Å, d and F are linearly dependent on D whereas E is quadratic in D, reflecting elastic behavior of the structure. On the retreat leg, where the rigid mount separation is increased starting from the zero strain state, all three quantities, d, E, and F, follow and extend the post-avalanche response observed during approach. The retreat leg reflects elastic behavior of the single structure practically up to a brittle-like failure (at D~3.3 Å), which occurs at roughly 20% tensile strain. This type of behavior, depicted on the retreat leg, is typical of the tensile response of defect-free solids [8].

The stepped-surface simulation predicts the presence of two avalanche events. As the structures are brought together, the first occurs when the partial plane abruptly moves from the tip surface to a position in which it is suspended midway between the bulk structures of the tip and sample. Here, the sample surface plane and first full surface plane of the tip display large out of plane distortions. Specifically, the portions of these planes in proximity to the partial plane are bowed outward, towards the interface. This event is marked by a small, precipitous drop in the structural energy at D=3.6 Å, as shown in Fig. 3. The absissa values in this case reflect the rigid mount separation minus the initial lengths of the tip structure (ignoring the partial plane) and the sample structure. As the separation is decreased further, the second avalanche occurs at D=1.6 Å when the adhesive forces between the sample surface plane and the first full surface plane of the tip causes them to move together abruptly. The resulting structure is bulk-like, with the partial plane embedded and forming a dislocation loop at its perimeter. As with the smooth-surface simulation results, the post-avalanche behavior (at D<1.6 Å) shows E displaying quadratic dependence on D, reflecting elastic behavior of the newly-formed single structure.

Along the retreat leg, elastic behavior is displayed by the structure up to a rigid mount separation value of roughly 2.1 Å where, unlike the smooth-surface case, this structure displays a gradual (rather than abrupt) trend

towards failure. Here, for D> 2.1 Å, dislocation multiplication proceeds from the site of the dislocation loop created by the presence of the partial plane embedded in the structure. The dislocation loop acts as a nucleation site for further noncatastrophic damage, typical of plastic deformation, which tends to mitigate abrupt failure. Thus, brittle failure along the retreat leg for the stepped-surface case is averted by the presence of the partial surface plane which posed as internal crystallographic damage once the adhesion process was completed.

DISCUSSION

The occurrence of avalanches in the adhesion process has been predicted for three different metals, at two crystallographic orientations, displaying either smooth or stepped surfaces. Although these results do not imply that this is a univeral phenomenon (i.e., regardless of material or surface geometry) they do suggest that adhesion, in many instances, will involve avalanches. As illustrated in Figs. 2 and 3, the post-avalanche behavior of the system is distinctly different than that displayed prior to avalanche. Indeed, the avalanche signals the transition from a system composed of two distinct structures to a single, strained structure. Thus, the transition, and consequently, the avalanche that signaled its occurrence (if abrupt), is perhaps the most crucial aspect of the adhesion process. Simulation results predict that, if heralded by the onset of an avalanche, the transition will occur over a period of less than 2 picoseconds. Unfortunately, current experimental techniques are unable to track the transition on this timescale. That is, the presence of an avalanche will necessarily define a regime where the interfacial separation is not controllable and the adhesive force is not measureable by means of AFM. In particular, with regard to the present case, the spike-like feature in Fig. 2c would not be detected by AFM, although the regions of the approach leg on either side of the force spike would be. Integration of AFM force data omitting the spike would miss the avalanche energy (i.e., the abrupt drop in structural energy associated with the avalanche). Thermodynamics defines the energy of adhesion as the sum of the energies of the isolated surfaces minus the energy of the interface resulting from adhesion. This definition, however, is not complete for strongly interacting materials, where the adhesion process includes the presence of adhesive avalanches. In this instance, we need to modify the definition to account for the avalanche energy, that is, adhesion energy equals total surface energy minus {interfacial energy + avalanche energy} [9]. Thus, without the ability to detect avalanche phenomena and thereby determine avalanche energy, AFM cannot be used as a quantitative tool in the study of surface and interfacial energetics whenever avalanche phenomena are present.

This work was supported by the U.S. Department of Energy under Contract No. DC-AC04-76DP00789.

REFERENCES

1. G. Binnig. C.F. Quate, and Ch. Gerber, Phys. Rev. Lett. 56, 930 (1986).
2. U. Dürig, O. Züger, and D.W. Pohl, Phys. Rev. Lett. 65, 349 (1990).
3. N.A. Burnham, D.D. Dominguez, R.L. Mowery, and R.J. Colton, Phys. Rev. Lett. 64, 1931 (1990).
4. E. Meyer, H. Heinzelmann, P. Grütter, Th. Jung, H.-R. Hidber, H. Rudin, and H.-J. Güntherodt, Thin Solid Films 181, 527 (1989).
5. S.A. Joyce and J.E. Houston, Rev. Sci, Instr. (in press).
6. J.R. Smith, G. Bozzolo, A. Banerjea, and J. Ferrante, Phys. Rev. Lett. 63, 1269 (1989).

7. S.M. Foiles, M.I. Baskes, and M.S. Daw, Phys. Rev. B 33, 7983 (1986).
8. A. Kelly, Strong Solids, 2nd ed. (Clarendon Press, Oxford, 1973).
9. P.A. Taylor, J.S. Nelson, and B.W. Dodson, (in preparation).

FIGURE CAPTIONS

Figure 1. Schematic representation of the initial geometry used in the simulations: (a) smooth-surface case; (b) stepped-surface case.

Figure 2. Smooth-surface simulations: (a) Interfacial separation d vs. rigid mount separation D; (b) structural energy E vs. D; and (c) adhesive force F vs. D. Attractive adhesive forces are negative. The absissa values are the rigid mount separation minus the initial lengths of the tip and sample structures.

Figure 3. Structural energy E vs. rigid mount separation D from the stepped-surface simulations. The absissa values are the rigid mount separation minus the initial lengths of the tip (ignoring the partial plane) and sample structures.

SIMULATION GEOMETRY

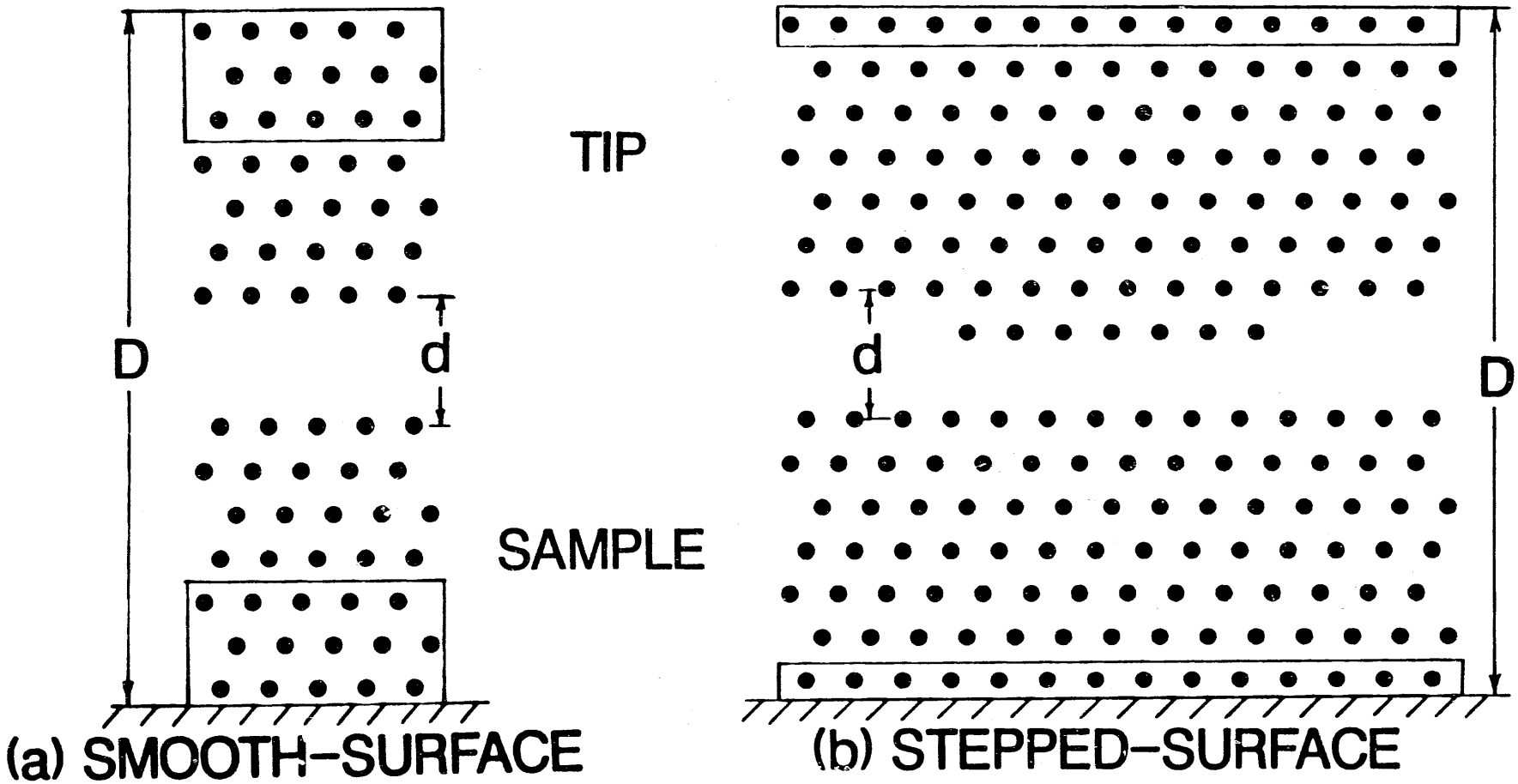

Fig. 1

SMOOTH–SURFACE Cu(111)

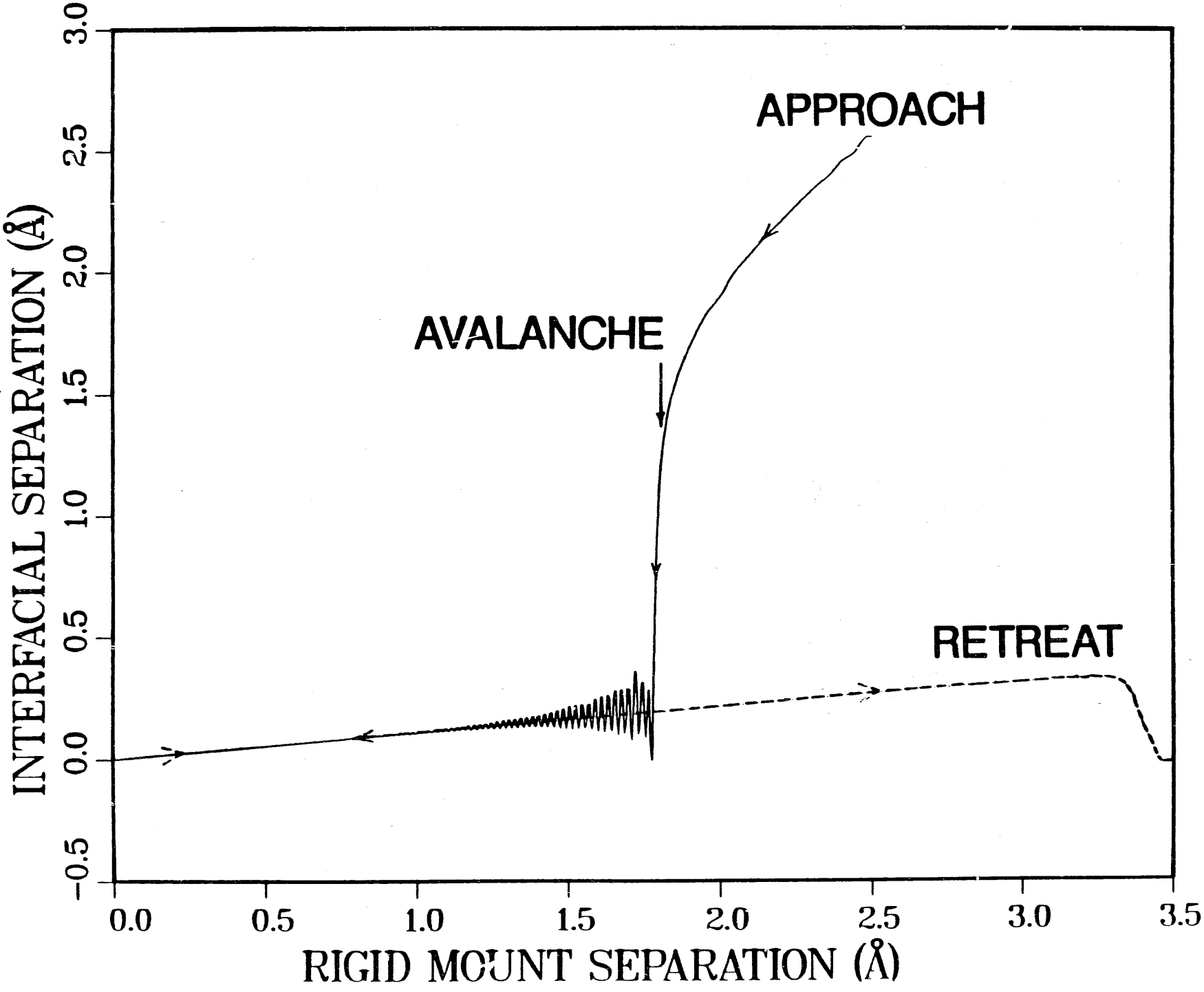

Fig. 2a

SMOOTH–SURFACE Cu(111)

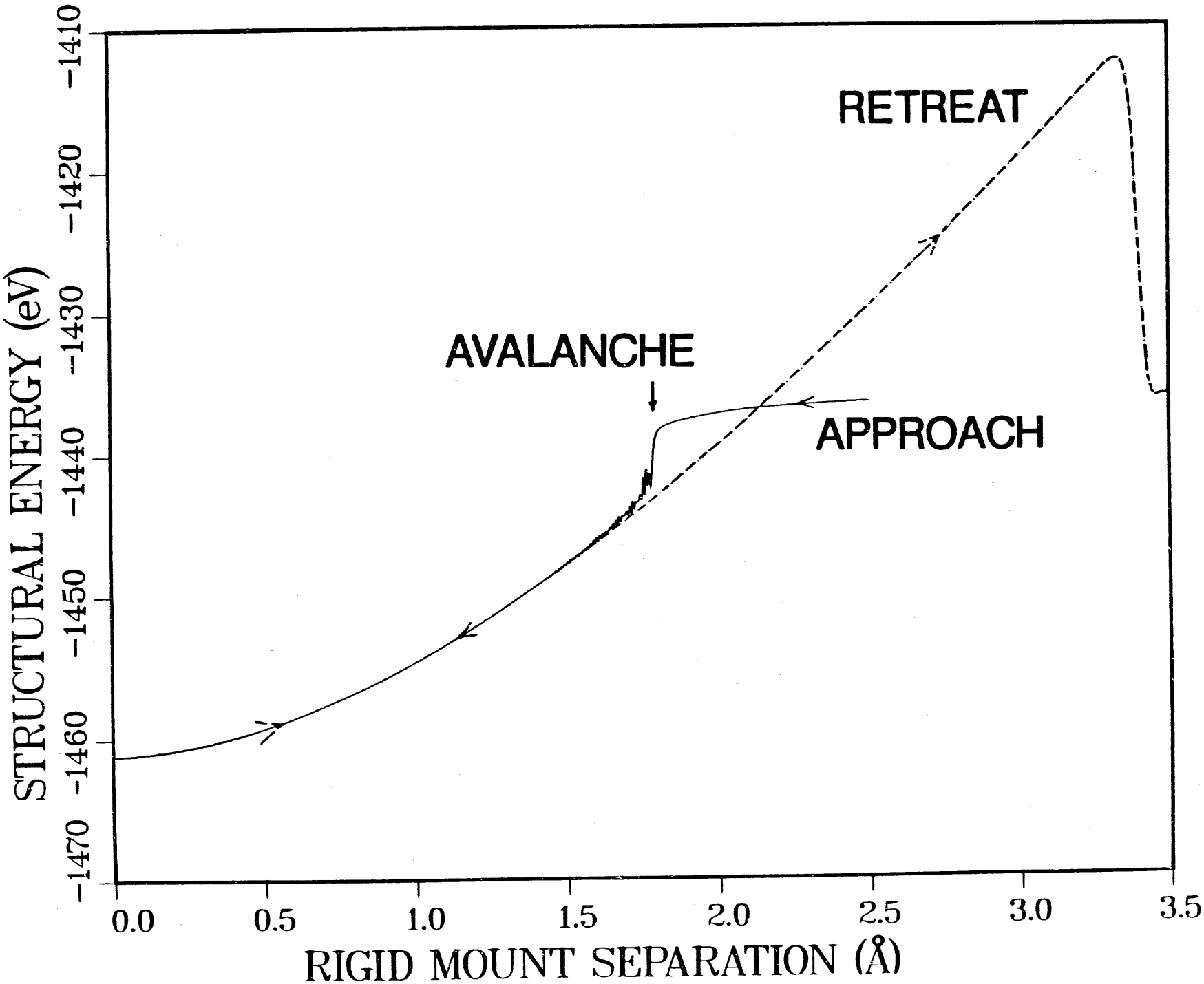

Fig. 2b

SMOOTH–SURFACE Cu(111)

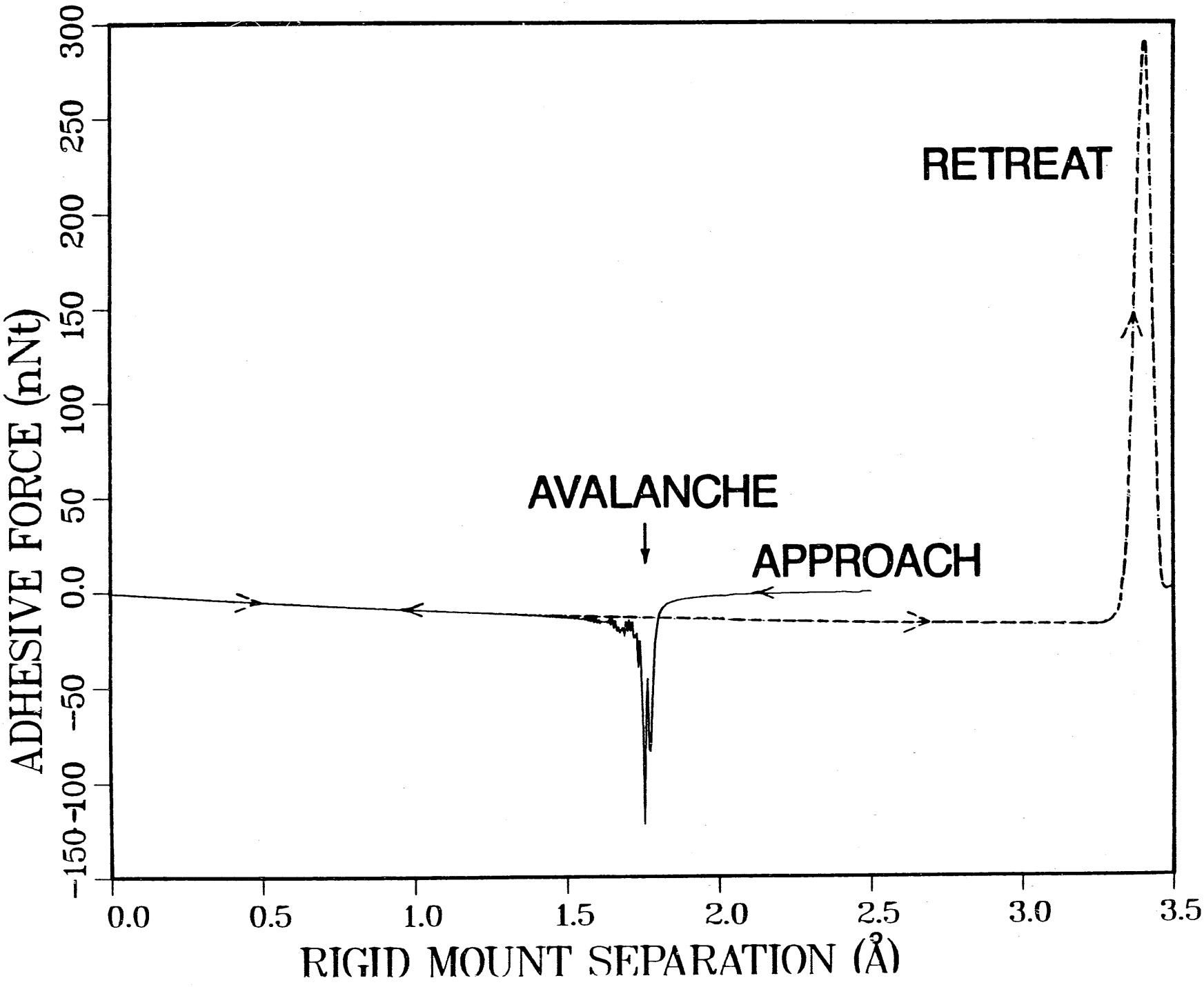

Fig 2c

STEPPED–SURFACE Cu(111)

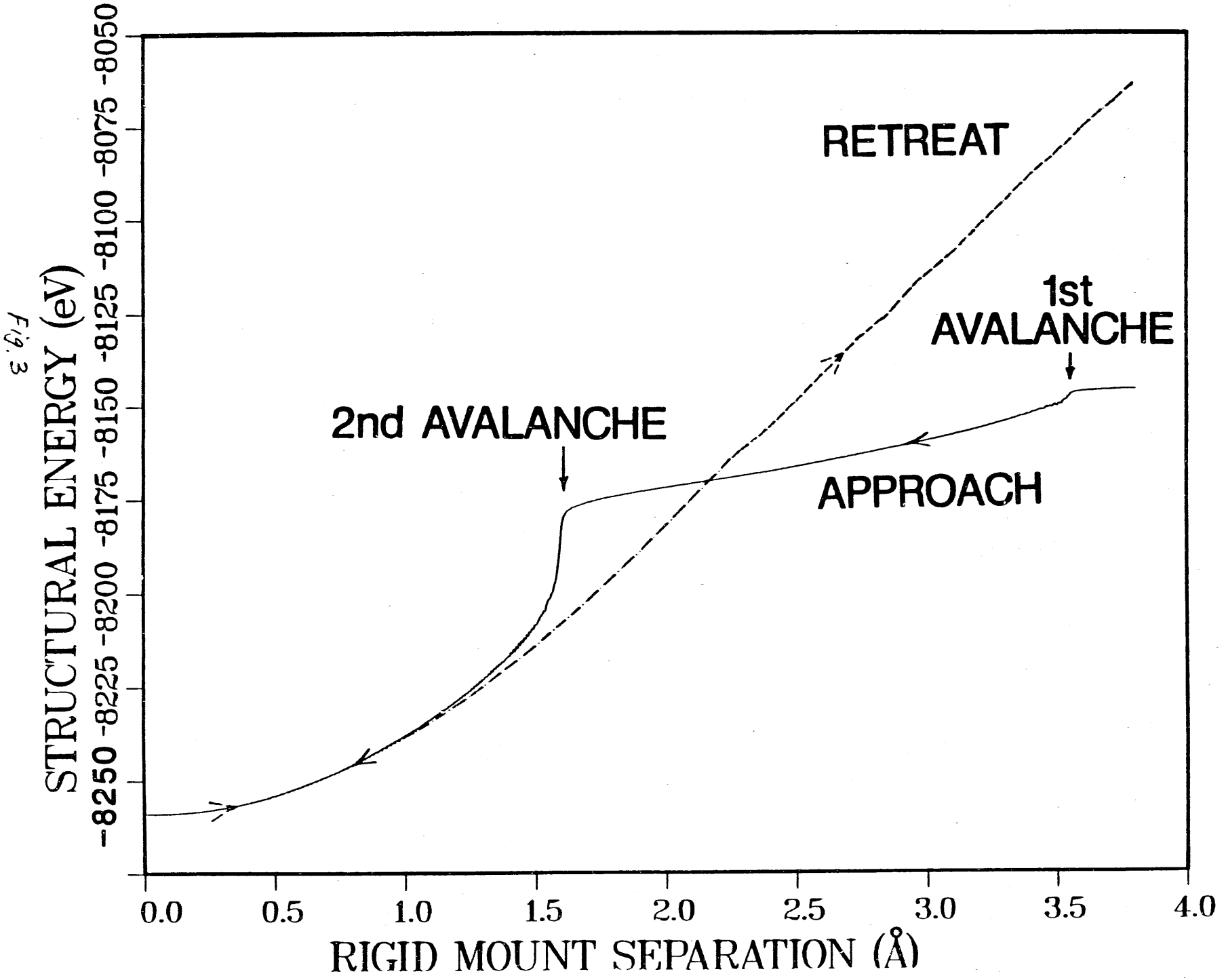

Fig. 3

END

DATE FILMED

12/28/90